*Acta Cryst.* (1955). 8, 22

# Cylindrical Patterson Functions for Collagen and Poly-γ-Methyl-L-Glutamate*

BY HARRY L. YAKEL, JR. AND PAUL N. SCHATZ†

*Gates and Crellin Laboratories, California Institute of Technology, Pasadena, California, U.S.A.*

(*Received* 1 *June* 1953)

Cylindrical Patterson projections for poly-γ-methyl-L-glutamate and collagen have been calculated from fiber diagram X-ray data with the aid of punched-card techniques. Interpretation of the observed functions is rather difficult owing to their poor resolution, which is caused in turn by the small amount of data available for inclusion in the calculations. A theoretical cylindrical Patterson projection for the 3·60 residue α-helix is also given. Qualitative comparisons indicate that the poly-γ-methyl-L-glutamate Patterson may be reasonably well explained on the basis of the α-helix structure, but that the collagen structure is probably quite different.

## Introduction

A method for the evaluation of a two-dimensional Patterson transform from the intensity distribution of a fiber diagram has been given by MacGillavry & Bruins (1948). Their discussion was based on the assumptions of strict periodicity in the fiber direction and completely random orientation of the chains around this axis. In a later treatment by Vineyard (1951), the former condition has been removed with a resultant generalization of MacGillavry & Bruins' equations.

An application of the method outlined in the earlier paper has been made with the X-ray diffraction data given by fibrous collagen and poly-γ-methyl-L-glutamate. A description of the method of calculation, an evaluation of the Patterson transforms obtained, and a brief comparison of these functions with a theoretical Patterson projection map for a 3·6 residue α-helix will be given in the following sections.

## Method of calculation

It was shown by MacGillavry & Bruins (1948) that a two-dimensional Patterson function $\varphi(z, x)$ for a periodic fiber with random azimuthal orientation can be defined by the equations

$$\varphi(z, x) = \sum_k \varphi_k(x) \cos 2\pi kz \,, \qquad (1)$$

$$\varphi_k(x) = \frac{2\pi}{NV} \int_0^\infty H(k, \xi) . J_0(2\pi\xi x) . \xi d\xi \,, \qquad (2)$$

where $z$ is the coordinate parallel to the fiber axis, $x$ is the radial distance of a point from the fiber axis, $\xi$ is the Bernal coordinate perpendicular to the fiber axis in reciprocal space, $k$ is the layer-line number introduced with the assumption of periodicity, $H(k, \xi)$ is the intensity distribution along the $k$th layer line, corrected for angular factors, $J_0(2\pi\xi x)$ is a zero-order Bessel function of the first kind for real arguments, $N$ is the number of periods in the fiber direction, and $V$ is the volume of the fiber irradiated.

The assignment of fiber repeat distances, and therefore values of $k$, to the collagen and poly-γ-methyl-L-glutamate structures has been a controversial matter. It seems clear, however, that, even if the distance selected for use in equation (1) is not the true repeat but only a pseudo-repeat, the Patterson function will still have most of the features of the true transform. The fiber repeat distances used in this calculation were 27·0 Å for poly-γ-methyl-L-glutamate and 29·3 Å for collagen. These repeats give indices 0, 2, 3, 5, 8, 10, etc. for the observable layer lines in the poly-γ-methyl-L-glutamate pattern, and 0, 3, 4, 5, 6, 7, 10, etc. for the observable layer lines in the collagen pattern.

The intensity distribution along the layer lines of a photograph of poly-γ-methyl-L-glutamate was measured with the aid of a Model B Eastman densitometer. The graph of the logarithm of the relative exposure time as a function of density given by Eastman Kodak for non-screen X-ray film (1947) was used to convert the observed data into relative intensities. Densitometer readings were taken at sufficiently close intervals so that a smooth intensity *v.* distance curve could be drawn through the observed points. Distances along the layer lines were expressed in the Bernal coordinate $\xi$ and Lorentz and polarization factors calculated in the usual manner were applied to the observed intensities to obtain finally the functions $H(k, \xi)$.

The collagen data were treated in an exactly analogous way, except that the intensities themselves were measured visually. In both cases the intensity distributions were measured along lines at values of $\zeta$ corresponding to separations $l/c$. Those portions of the reflections which were off the layer lines, owing to the arcing effect produced by disorientation, were neglected. If these were to be incorporated into the cal-

* Contribution No. 1810 from the Gates and Crellin Laboratories.

† Frank B. Jewett Postdoctoral Fellow of the American Telephone and Telegraph Company.

culations, the more complicated expressions of Vineyard (1951) would have to be used.

The coefficients $\varphi_k(x)$ for both problems were calculated from the intensity distributions with the use of punched-card methods. Values of $H(k, \xi)$, $k$ and $\xi$ were punched into a set of detail cards, and arguments $2\pi\xi x$ were calculated for values of $x$ ranging from 0 to 8·0 Å at intervals of 0·4 Å for collagen and 0·2 Å for poly-$\gamma$-methyl-L-glutamate. Zero-order Bessel functions corresponding to the arguments were gang-punched into the detail cards from a master deck* and the integrands $H(k, \xi).J_0(2\pi\xi x).\xi$ were computed with an International Business Machines 604 electronic calculating unit. The integrations were performed numerically with the same machine. The calculation extended over layer lines with index 0, 3, 4, 5, 6, 7 and 10 for collagen and 0, 2, 3, 5, 8 and 18 for poly-$\gamma$-methyl-L-glutamate.

The final summation of the two-dimensional Patterson functions was carried out with Beevers–Lipson strips, as indicated in equation (1). The series were put on an approximate absolute scale by adding constant positive backgrounds equal in magnitude to the largest negative values reached by the functions.

## Interpretation of the Patterson functions

The two-dimensional Patterson projections obtained for collagen and poly-$\gamma$-methyl-L-glutamate are shown in Fig. 1(*a*) and Fig. 1(*b*) respectively. It should be noted that the functions actually shown in these figures are $\varphi(z, x).x$. Multiplication by the Patterson coordinate perpendicular to the fiber axis was suggested by consideration of the relation between a cylindrically projected three-dimensional Patterson function, independent of azimuth angle $\alpha$, and a two-dimensional function of the type derived by MacGillavry & Bruins (1948). Support for this procedure was later found in a calculation of the theoretical shape assumed by a Gaussian Patterson peak in three-dimensional space when projected cylindrically (Yakel, 1953).

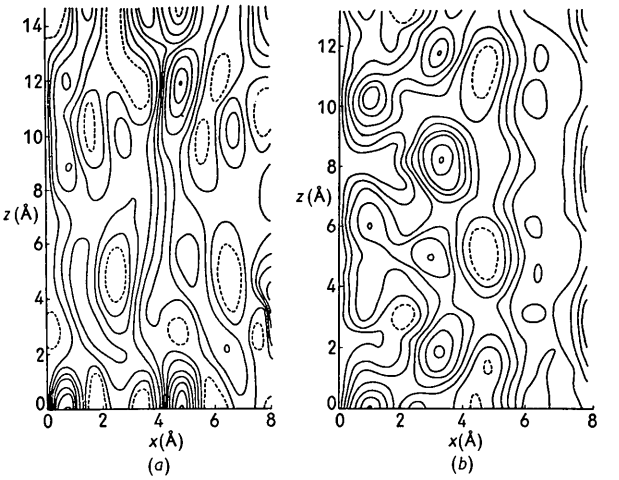


Fig. 1. (*a*) Observed cylindrical Patterson function for collagen. (*b*) Observed cylindrical Patterson function for poly-$\gamma$-methyl-L-glutamate.
Contours shown are at arbitrary, equally separated levels. Areas inside broken contours represent minima of the function.

It is clear that the resolution of both Patterson functions is very poor, the reason probably being that the data used in the series did not extend to large values of $\sin\theta/\lambda$. A discussion of these functions in terms of detailed models of the polypeptide chain is not possible, but several general features are worthy of note.

The presence of peaks of fairly large magnitude about 1 Å from the fiber axis is common to both projections. These peaks may be partially an artifact, however, owing to the lack of data and disorientation in the packing of the polypeptide molecules. The peaks seem to arise experimentally from the relatively high intensity of the equatorial reflections obtained from both collagen and poly-$\gamma$-methyl-L-glutamate. Inspection of equations (1) and (2) shows that if these large intensities are not counterbalanced by a large amount of data from higher layer lines they will insure the presence of high peaks at $x = 0$ in $\varphi(z, x)$, or slightly displaced from the fiber axis in $\varphi(z, x).x$.

The experimentally observed high intensities of the equatorial layer lines relative to the higher layer lines may be produced by randomness in the vertical stacking of the individual peptide molecules which would contribute to a general decrease in non-equatorial layer-line intensities while leaving the equatorial intensities unaffected.

The rows of peaks roughly parallel to the fiber axis along the lines $x \cong 5{\cdot}0$ Å in Fig. 1(*a*) and $x \cong 3{\cdot}2$ Å in Fig. 1(*b*) may be interpreted as arising from interactions between atoms of different molecules or, in the case of poly-$\gamma$-methyl-L-glutamate, from interactions between atoms of the peptide chain and side chain atoms. An interesting alternative explanation may be advanced if helical chains similar to those proposed by Pauling, Corey & Branson (1951) are

* The master deck of zero-order Bessel functions $J_0(y)$ used in these calculations covers the range of arguments 0 to 20·000 at intervals of 0·004 in the argument. The deck was prepared by direct calculation of the functions with the aid of the following relationships, which can be derived from formulas involving the derivatives of zero and first-order Bessel functions,

$$J_0(y_{n+1}) = J_0(y_{n-1}) - 2\Delta y . M_1(y_n)/y_n , \quad (3)$$

$$M_1(y_{n+2}) = M_1(y_n) + 2\Delta y . y_{n-1} J_0(y_{n-1}) . \quad (4)$$

Here $\Delta y = 0{\cdot}002$, $n$ is given by the equation $y_n = 0{\cdot}002.n$, and $M_1(y_n) = y_n J_1(y_n)$. With a suitably planned program board for the 604 calculating unit, it was possible to compute $J_0(y)$ to $y = 20{\cdot}000$ merely by introducing the values of $J_0(0{\cdot}000)$ and $J_1(0{\cdot}002)$ on a lead card, the machine performing all subsequent operations as indicated in (3) and (4) and punching the resultant Bessel functions and arguments into a set of trailer cards. The functions were calculated to four significant figures after the decimal point with a maximum error of $\pm 0{\cdot}0002$ and an average error much less than 0·0001.

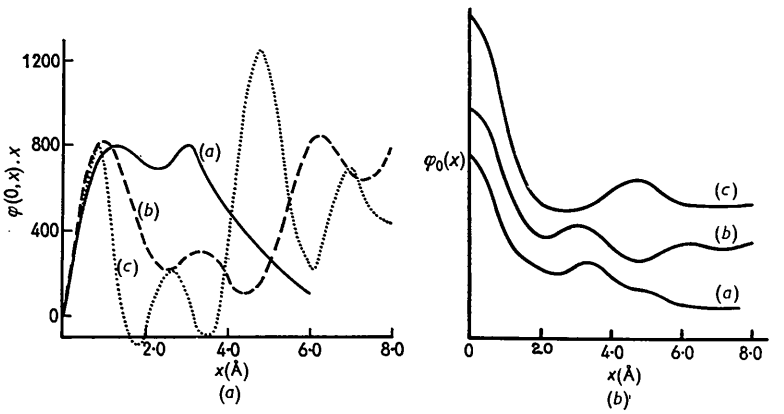


Fig. 2. (*a*) $\varphi(0, x).x$ functions for the compounds studied, with the functions placed on the same arbitrary relative scale. Full curve (*a*) is taken from theoretical cylindrical Patterson function for 3·60 residue $\alpha$-helix. Dashed curve (*b*) is taken from observed Patterson for poly-$\gamma$-methyl-L-glutamate. Dotted curve (*c*) is taken from observed Patterson for collagen. (*b*) $\varphi_0(x)$ functions for the compounds studied. The function have been placed on the same arbitrary relative ordinate scale and the axis of ordinates has been displaced upward for curves (*b*) and (*c*) to make comparison easier. Curve (*a*) was obtained from the interatomic distances of the 3·60 residue $\alpha$-helix, curve (*b*) was obtained from the X-ray data for poly-$\gamma$-methyl-L-glutamate, and curve (*c*) was obtained from the X-ray data for collagen.

assumed to be present. The rows of peaks under consideration might then be attributed to interactions between atoms located on opposite sides of the same helix. That is, the distance of these peaks from the fiber axis, corrected for the shift in peak position with cylindrical projection, would be a measure of the diameter of the helix.

It is not immediately evident that interatomic distances with values of $\Delta x$ equal to the helix diameter would be so numerous as to produce a chain of Patterson peaks separated from the fiber axis by a definite minimum. This minimum may be exaggerated, however, owing to diffraction effects surrounding the peaks near the fiber axis. In this case a general distribution of maxima could be considered as extending to $x = 3{\cdot}2$ Å (poly-$\gamma$-methyl-L-glutamate) or 5·0 Å (collagen), and the interpretation of the latter values in terms of average helix diameter would seem more reasonable.

The 3·0 Å diameter which in this way would be associated with the helical poly-$\gamma$-methyl-L-glutamate molecules is in fairly good agreement with the value predicted from the 3·60 residue $\alpha$-helix. The 4·8 Å diameter for collagen would indicate a more open spiral, resembling in this respct the three-strand helix proposed for this substance by Pauling & Corey (1951*a*, *b*).

Fig. 2(*a*) shows the functions $\varphi(0, x).x$ for the two compounds. The maximum at about 2·7 Å in the curve for collagen may be a false diffraction peak but may also represent inter-chain van der Waals or hydrogen-bonded contacts. The pronounced maximum at 6·1 Å for poly-$\gamma$-methyl-L-glutamate can be attributed to interactions such as those between main-chain atoms of one helix and the side-chain atoms of an adjacent helix. Fig. 2(*b*) shows the functions $\varphi_0(x)$ which are equivalent to radial distribution functions of the projections and which should therefore contain information about the lateral packing of the polypeptide chains. A theoretical $\varphi_0(x)$ function calculated with the atomic parameters for the 3·60 residue $\alpha$-helix given by Pauling & Corey (1951*a*, *b*) is also shown in Fig. 2(*b*). It is seen that the experimental curve for poly-$\gamma$-methyl-L-glutamate resembles in gross details this calculated function while the curve for collagen is significantly different.

A theoretical cylindrical Patterson projection obtained from the interatomic distances in a 3·60 residue $\alpha$-helix by the method described by Yakel (1953) is given in Fig. 3. Only main-chain and $\beta(1)$ carbon atoms were used to calculate this function, which extends over all eighteen amino-acid residues in a

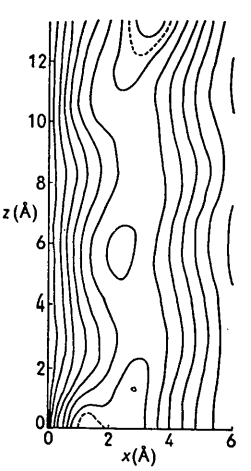


Fig. 3. The theoretical cylindrical Patterson function for the 3·60-residue $\alpha$-helix. Contours are shown at intervals of 100. The broken contours indicate the 750 level. This function was calculated from only those atomic interactions involving main-chain and $\beta$ carbon atoms of the 18 residues in a repeat of this helix.

fiber repeat. A temperature function corresponding to $B = 30$ Å$^2$ was used in the computation. This temperature factor is probably too large by about 5 Å$^2$ but the general character of the Patterson function would not be changed materially by this correction. A comparison of the theoretical function with the two experimental Pattersons shows that only a few general conclusions can be drawn as to the possible applicability of an $\alpha$-helix model to the structures which the Patterson diagrams represent. The dissimilarity between the calculated projection and the Patterson diagram for collagen indicates that it is improbable that single $\alpha$-helices are major structural components of that compound. There are some points of similarity with the poly-$\gamma$-methyl-L-glutamate function, particularly in the region of the line $x \cong 3{\cdot}0$ Å. The main point of disagreement between these two functions is the absence of any well distinguished peaks along the line $x \cong 1{\cdot}0$ Å in the theoretical function. This probably reflects the fact that the peaks at $x \cong 1{\cdot}0$ Å in the observed functions are artifacts or the result of disorientations in the structure which were not duplicated in the theoretical function. The line $\varphi(0, x).x$ from the calculated projection is included in Fig. 2(*a*) for purposes of comparison with the experimental curves. In all comparisons between the observed and theoretical functions at large $x$ values it must be kept in mind that no side-chain atoms, other than a $\beta$ carbon atom, were included in the latter. The general rise of the observed functions for values of $x$ greater than 5 Å is of course due to main-chain, side-chain and interchain interactions, which appear to be more and more important because of the weighting on $x$.

## Conclusion

It has been found that cylindrical Patterson functions calculated from relatively meager X-ray data given by a fibrous protein and a synthetic poly-peptide yield only general, semi-quantitative information about the structures of these compounds. More detailed conclusions might be reached if the resolution of the projections were improved; this might be achieved by the inclusion of more intensity data at shorter spacings.

We would like to thank Dr S. Frankel and Mr W. Chaplin of the Digital Computing Laboratory for their assistance in planning those phases of the calculations which involved punched card methods.

This work was supported in part by Contract Nonr 220(05) between the California Institute of Technology and the Office of Naval Research.

## References

MacGillavry, C. H. & Bruins, E. M. (1948). *Acta Cryst.* **1**, 156.

Pauling, L. & Corey, R. B. (1951*a*). *Proc. Nat. Acad. Sci., Wash.* **37**, 235.

Pauling, L. & Corey, R. B. (1951*b*). *Proc. Nat. Acad. Sci., Wash.* **37**, 272.

Pauling, L., Corey, R. B. & Branson, H. R. (1951). *Proc. Nat. Acad. Sci., Wash.* **37**, 205.

*Radiography in Modern Industry* (1947). Rochester: Eastman Kodak Company, X-ray Division.

Vineyard, G. H. (1951). *Acta Cryst.* **4**, 281.

Yakel, H. L., Jr. (1953). *Acta Cryst.* **6**, 724.

*Acta Cryst.* (1955). **8**, 25

# The Structure of Titanium Oxydifluoride

By Karl Vorres and Jerry Donohue

*Department of Chemistry, University of Southern California, Los Angeles, California, U.S.A.*

(*Received* 19 *July* 1954)

The structure of titanium oxydifluoride, $TiOF_2$, has been determined from X-ray powder photographs. The structure consists of titanium atoms octahedrally coordinated by randomly distributed oxygen and fluorine atoms, these octahedra sharing all six corners with neighboring octahedra. It is shown that powder data previously attributed to $TiF_4$ are probably due to $TiOF_2$.

## Experimental

In the course of a study of various halides of titanium, titanium oxydifluoride, $TiOF_2$, was obtained as the product of hydrolysis of titanium tetrafluoride; it was also prepared by the hydrolysis of titanium trifluorochloride, and from the reaction of aqueous or anhydrous hydrogen fluoride with titanium dioxide (Vorres & Dutton, 1954). The oxydifluoride, when purified, was a white powder. The various methods of preparation did not give any single crystals. Powder specimens were sealed in glass capillaries and photographed in a Straumanis-type camera with filtered Cu $K\alpha$ radiation, $\lambda = 1{\cdot}542$ Å. Relative intensities